Temporal and Angular Resolution of the Ionization-Induced Refraction of a Short Laser Pulse in Helium Gas

P. Chessa,[2,3,*] E. De Wispelaere,[1] F. Dorchies,[1] V. Malka,[1] J. R. Marquès,[1]
G. Hamoniaux,[2] P. Mora,[3] and F. Amiranoff[1]
[1]*LULI; UMR 7605, CNRS-CEA-Ecole Polytechnique-Université Paris VI; Ecole Polytechnique, 91128 Palaiseau, France*
[2]*Laboratoire d'Optique Appliquée, ENSTA; Ecole Polytechnique, 91128 Palaiseau, France*
[3]*Centre de Physique Théorique, CNRS, Ecole Polytechnique, 91128 Palaiseau, France*
(Received 27 July 1998)

The refraction of a short and intense laser pulse focused in helium gas has been studied both experimentally and numerically. Using the time-frequency correspondence of a 120 fs laser pulse linearly chirped to 1.8 ps, the ionization-induced refraction is resolved both temporally and angularly. Two-dimensional numerical simulations are performed to calculate the laser propagation, from the focusing lens to the detector. With such a simulation, we get a quantitative agreement with the experiment, both for the refraction of the chirped pulse and for the ionization-induced blueshifted spectrum of the compressed pulse. [S0031-9007(98)08310-0]

PACS numbers: 52.40.Nk, 52.25.Jm, 52.50.Jm, 52.65.–y

Understanding the physical mechanisms governing the propagation of intense ($\geq 10^{16}$ W/cm^2) ultrashort (≤ 1 ps) laser pulses in a gas is a crucial issue for applications such as x-ray lasers [1,2], high-harmonic generation [3], and particle acceleration [4]. With such pulses, optical-field-induced ionization causes a rapid increase in the electron plasma density on the laser axis and hence a decrease of the refractive index in time and space. The plasma-induced self-phase-modulation leads to the complementary effects of spectral blueshifting and beam refraction. This last effect decreases the laser intensity at focus, which in some cases, leads to a decrease of the ionization state. Laser-plasma interaction at both high intensity and high electron density is then more difficult [5], if not impossible.

The ionization-induced blueshift has been predicted by Wilks *et al.* [6] and first observed by Wood and co-workers [7]. In another experiment [8], they have time resolved the blueshift of a probe pulse propagating with the gas-plasma interface produced by a pump pulse. Ciarroca *et al.* [9] have spatially resolved the blueshifted spectrum across the focal plane and compared their results with a two-dimensional numerical propagation model [10]. More recently, Le Blanc and Sauerbrey [11] have temporally and spatially measured the spectral blueshifting.

The ionization-induced refraction has been predicted by Rankin *et al.* [12] and confirmed by numerical simulations [12–14]. The experimental demonstration has been performed by Auguste *et al.* [15,16]. They have measured the longitudinal displacement of the focal plane induced by beam refraction and the increase of the size of the focal spot. Their results have been compared with analytical models [15,17]. Nevertheless, no information on which temporal part of the pulse is refracted is available.

In all these experiments, no quantitative agreement with simulations has been obtained, for the blueshifted spectra as well as for refraction. As a matter of fact, such a comparison is impossible without simulating the full experiment, including the laser propagation from the interaction region up to the detector.

In this Letter, we present an experiment where we have temporally and angularly resolved the ionization-induced refraction. These results and also the ionization-induced blueshifted spectra, are, for the first time, to our knowledge, quantitatively and successfully compared with simulations. We have thus the possibility of fully understanding the evolution of the laser pulse during its propagation.

The experiment was performed at the Laboratoire d'Optique Appliquée with a CPA (chirped pulse amplification) 10 Hz Ti:sapphire laser [18]. It delivers pulses of 30 mJ maximum energy, 120 fs FWHM (full width at half maximum) minimum duration, with a 10 nm FWHM spectrum centered at 800 nm. Two spherical mirrors in the Bowen configuration focus at $f/4.4$ the 25 mm diameter beam in the middle of a chamber filled with helium gas. The focal spot has a radius at $1/e^2$ in intensity of 4.2 μm and contains 70% of the incident energy, giving a maximum laser intensity of 6×10^{17} W/cm^2. The laser beam coming out of the interaction region is collected by a $f/2.4$ doublet ($f = 12$ cm) and sent into a spectrometer coupled to a 8 bit linear charge-coupled device (CCD) camera. The spectral resolution is 2.5 nm.

In order to compare our experimental results with theory, we performed simulations with the code WAKE and the numerical diagnostic tool called IMAGE [19,20]. WAKE is a cylindrical two-dimensional particle code simulating the interaction of short laser pulses with atomic gas and/or plasmas. It is applicable for underdense plasmas (laser frequency ω_0 higher than the electron plasma frequency ω_p), for laser intensities ranging from 10^{14} W/cm^2 up to the relativistic regime, and in the quasistatic limit (typical time of nonlinear reshaping of the pulse long compared

 0031-9007/99/82(3)/552(4)$15.00

to the plasma period $2\pi/\omega_p$). The wave equation solved by WAKE allows wide spectrum laser pulses. According to this wave equation any spectral component of the pulse propagates within a spectrally adapted paraxial approximation. The ionization is included by means of a tunneling rate obtained from a quasiclassical model for a hydrogen atom in a static electric field [21] and extended to any high-Z atom [22]. A phenomenological correction to these rates [23] is taken into account in order to extend them to small atoms. WAKE simulates the interaction up to the point after the laser focus where no ionization occurs any more. Light then propagates as in vacuum.

The spectrum of the transmitted light at the detector plane is the result of interference between light at different frequencies, emerging from the plasma at different radial positions with different angles and phases. It cannot be calculated correctly without taking into account the details of the imaging system, including its finite aperture. This is why the postprocessor IMAGE [19] simulates the propagation of light emerging from the plasma up to the detector plane through the collecting optics. It then calculates the spectrum at the detector plane. It uses a spectrally adapted paraxial approximation consistent with WAKE. With these two codes we are able to simulate the laser gas/plasma interaction over the pulse waist region with submicron resolution and to analyze the transmitted pulse far away from the plasma, at the detector position.

In a first step, to demonstrate the accuracy of our theoretical model, we have compared our simulations with experimental ionization-induced blueshifted spectra. These spectra were obtained by imaging the focal plane on the spectrometer slit. Figure 1 presents the experimental and numerical spectra obtained by focusing the compressed (120 fs, 6×10^{17} W/cm^2) pulse in helium gas at different pressures. The spectral width, shift, and modulations increase with pressure. The undisturbed (vacuum) spectrum has a Gaussian profile centered at 800 nm. In the simulation, the incident spectrum corresponds to a pulse duration of 120 fs, which implies a spectral width of 6 nm. This does not match perfectly the experimental value (10 nm). This means that a temporal phase perturbation existing in the real pulse is neglected in the simulations. The effect of such an approximation would be visible only for very low gas pressures where the broadening of the spectrum due to ionization is negligible. In our conditions, the spectral broadening due to ionization is much larger than the original difference between the experiment and the simulation.

We observe from Fig. 1 that the agreement between measured and simulated spectra is very good, with a difference smaller than 13% on the width $\Delta\lambda = \sqrt{\langle\lambda^2\rangle - \langle\lambda\rangle^2}$, and 33% on the wavelength shift $\delta\lambda = \langle\lambda\rangle - \lambda_0$, where $\langle\lambda\rangle$ is the mean wavelength.

In a second step we resolved the ionization-induced refraction in time and angle. The time resolution is obtained by initially chirping the pulse in frequency (by changing the distance between the two gratings of the compressor). With such a linearly chirped pulse, each temporal slice corresponds to a frequency slice in the spectrum: $\omega(t) = \omega_0 + \alpha t$, where $\omega(t)$ is the instantaneous laser frequency and the temporal origin is taken at the laser pulse maximum. By recording the frequency-angle spectrum of the pulse leaving the interaction region, a temporal resolution of the refraction undergone by the laser beam at the gas-plasma interface is thus obtained.

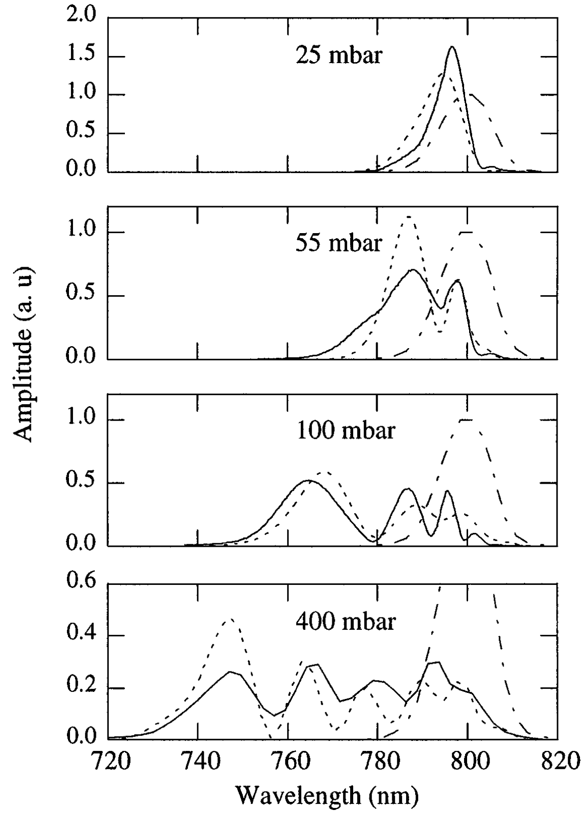

FIG. 1. Ionization-induced blueshifted spectra after interaction different of helium gas pressures. Plain line: experiment; dashed line: simulation; dash-dotted line: spectrum in vacuum of the simulated pulse.

For the angular resolution, the collecting lens was adjusted to collimate the outgoing beam. In this case, the transverse position on the collecting lens r gives the angle $\theta = \tan^{-1}(r/f)$ between the laser ray and the propagation axis. Before entering the spectrometer, a telescope adjusts the beam diameter to the vertical width of the CCD.

Figure 2 presents results obtained at a pressure of 375 mbar and a FWHM pulse duration of 1.8 ps ($|\alpha| \approx$ 16 ps^{-2}; maximum intensity of 4×10^{16} W/cm^2). Figure 2(a) shows the angular distribution (transverse profile) of the transmitted beam. It was obtained with the spectrometer slit fully opened (left and right edges of the image) and by recording the zero order of the grating. Figures 2(b) and 2(c) have been obtained by narrowing the spectrometer slit and looking at the first order. They show the frequency (time) resolution of this angular distribution in the case of a positive chirp (large wavelengths

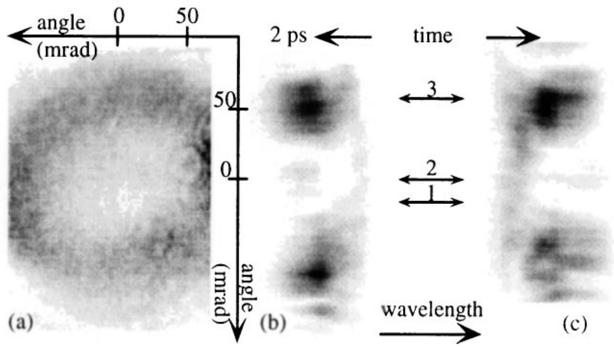

FIG. 2. (a) Angular (transverse) profile of the chirped laser pulse at the collecting lens plane without frequency resolution (beam profile), with frequency (time) resolution and a (b) positive or (c) negative chirp. The helium gas pressure is 375 mbar.

at the front part of the pulse) or a negative chirp, respectively. Under vacuum (without ionization-induced effects) both the spatial and the spectral distributions are Gaussian. When the gas pressure is increased, the ionization-induced refraction becomes more and more effective and modifies the beam profile. This is clearly illustrated by Fig. 2(a) where the initially Gaussian beam leaves the interaction region with a ring shape.

Lineouts of Figs. 2(b) and 2(c) are presented in Fig. 3. Lineouts at positions 1 and 2 show that most of the spectrum has disappeared from the laser axis. Only the front part of the pulse [long wavelengths in Fig. 3(a); short wavelengths in Fig. 3(b)] is still present after the interaction. The frequency cutoff arises about 1 ps before the laser pulse maximum. With a maximum laser intensity of 4×10^{16} W/cm^2, this corresponds to an intensity of about 1.7×10^{16} W/cm^2, close to the ionization threshold of He^{2+}. Lineouts at position 3 show that the spectrum in the ring is broader for the negative chirp (blue before red) than for the positive chirp.

To compare these results with theory, we have simulated the chirped pulse interaction using the code WAKE and we have worked out the near-field space resolved spectrum with the postprocessor IMAGE. For this particular case, IMAGE is configured to calculate the near-field

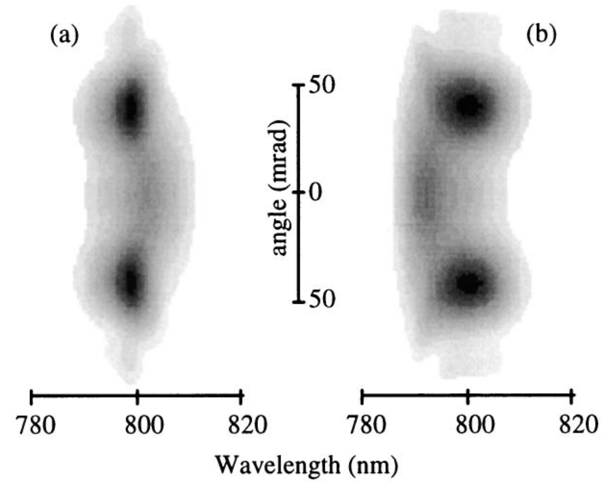

FIG. 4. Numerical simulations of the frequency (time) resolved angular (transverse) profile of a chirped laser pulse 12 cm after the focal plane, and with a (a) positive or (b) negative chirp. Same laser and gas parameters as in Fig. 3.

propagation of the pulse in vacuum at many centimeters from the plasma. A quadratic phase variation in time, i.e., a linear increase of frequency, has been added to the Gaussian longitudinal shape of the 1.8 ps pulse. The phase variation is chosen to match the 10 nm spectral width of the experimental pulse. All the non-quadratic-phase perturbations have been neglected.

Figure 4 shows two spectra, obtained with opposite chirps and the same laser and gas parameters as for the experimental results of Figs. 2 and 3. Lineouts of Fig. 4 are presented in Fig. 5. The same features are visible in the simulation and in the experimental spectra: After interaction with the gas, the front part of the pulse keeps its maximum intensity on the axis, while the rest of the pulse leads to an annular profile. As in the experiment (Fig. 3, position 3), the spectral width of the ring is smaller for the positive chirp than for the negative chirp.

From Figs. 2, 3, and 4 we conclude that the interaction scenario is the following: The front part of the pulse that has an intensity below the ionization threshold propagates in the gas as in vacuum and is not modified. This lasts

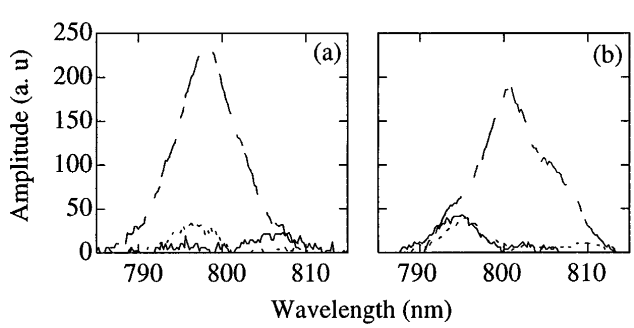

FIG. 3. (a) and (b): Lineouts of Figs. 2(b) and 2(c), respectively, for positions 1 (full line), 2 (dotted line), and 3 (dashed line) of Fig. 2.

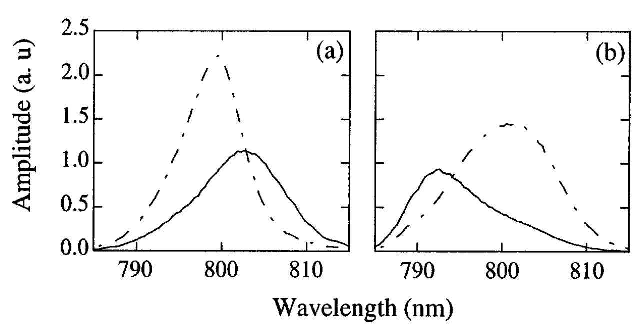

FIG. 5. (a) and (b): Lineouts of Figs. 4(a) and 4(b), respectively, on the axis (full line, position 2) and 42 mrad from the axis (dashed line, position 3).

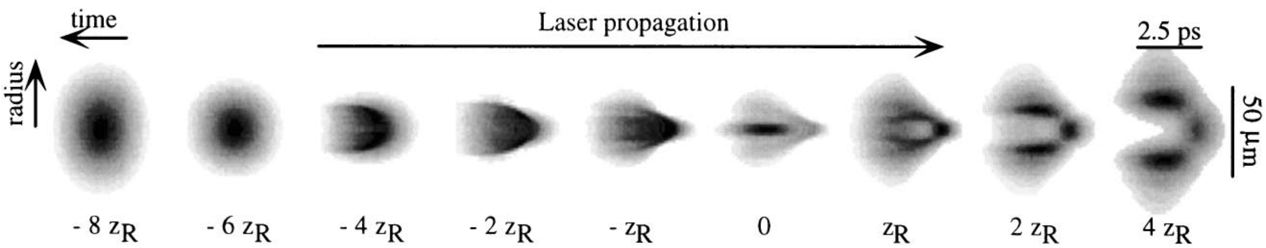

FIG. 6. Spatiotemporal evolution of a 1.8 ps linearly chirped laser pulse propagating in helium gas.

until the intensity becomes high enough for the ionization rate to take effect. Because the initial transverse intensity profile is Gaussian, the ionization starts on the laser axis first and creates a steep electron density gradient at the gas-plasma interface. The associated refractive index gradient acts as a negative lens that deflects the laser rays away from the laser axis. Moreover, the rapid increase in electron density tends to blueshift the laser rays. The rest of the pulse is then refracted away from the propagation axis by the gas-plasma interface. Because the ionization occurs early in the pulse, it is the leading part of the pulse that is spectrally blueshifted, as observed by [8,11]. So, the spectrum of a positively chirped pulse (red before blue) will be compressed by the interaction, whereas the spectrum of a negatively chirped pulse (blue before red) will be broadened. This is observed on the spectra in the rings in Fig. 4.

The interaction scenario is illustrated by the simulation presented in Fig. 6. The pulse evolution is shown at steps of one or two Rayleigh lengths z_R ($\approx$70 μm). Despite the defocusing effect due to ionization, the pulse still focuses at about the focal plane in vacuum ($z = 0$). However, at this point, the shape has changed to a weak, detached front part followed by a radially modulated main part having a first maximum on axis and a weaker one on a ring. Further in the propagation, the front part propagates as in vacuum, while the main part is pushed away from the axis by refraction ($z = z_R$). At $z = 2z_R$, the central part has been already completely refracted away from the axis, leading to a well defined annular shape. From this point, the laser intensity becomes too low to ionize the gas and the propagation is just governed by diffraction. These numerical results agree with the theoretical investigation made by Lontano *et al.* [24] on the interaction between a strong ionizing laser pulse and an initially neutral gas. Our experimental results give the first demonstration of these simulations, both of the spatial and the frequency evolution of the laser pulse.

In conclusion, we have studied the interaction of a short linearly chirped laser pulse with helium gas. Using the time-frequency correspondence in the pulse, we have performed the first temporal resolution of the ionization-induced refraction. The laser gas/plasma interaction as well as the optical diagnostic has been simulated using the codes WAKE and IMAGE, respectively. By working out the laser propagation and interaction from the focusing lens to the detector plane, we have been able to make not only a qualitative but also a quantitative comparison between experiment and theory. Without any adjustable parameter, we obtain a very good agreement, both for the beam refraction and the ionization-induced blueshift. Such numerical tools allow fine comparisons with experimental data and are of great interest for the design of experiments.

This work has been supported by the European Community large facility program under Contract No. CHGE CT930021.

*Permanent address: IFAM-CNR, Via del Giardino 7, 56100, Pisa, Italy.

[1] N.H. Burnett and P.B. Corkum, J. Opt. Soc. Am. B **6**, 1195 (1989).
[2] D.C. Eder *et al.*, Phys. Rev. A **45**, 6761 (1992).
[3] A. l'Huillier *et al.*, Phys. Rev. A **46**, 2778 (1992).
[4] E. Esarey and P. Sprangle, IEEE Trans. Plasma Sci. **24**, 252 (1996).
[5] V. Malka *et al.*, Phys. Plasmas **3**, 1682 (1996).
[6] S.C. Wilks *et al.*, Phys. Rev. Lett. **61**, 337 (1988).
[7] Wm. M. Wood *et al.*, Opt. Lett. **61**, 337 (1988).
[8] Wm. M. Wood *et al.*, Phys. Rev. Lett. **67**, 3523 (1991).
[9] M. Ciarroca *et al.*, Opt. Commun. **110**, 425 (1994).
[10] S.C. Rae, Opt. Commun. **104**, 330 (1994).
[11] S.P. Le Blanc and R. Sauerbrey, J. Opt. Soc. Am. B **13**, 72 (1996).
[12] R. Rankin *et al.*, Opt. Lett. **16**, 835 (1991).
[13] W.P. Leemans *et al.*, Phys. Rev. A **46**, 1091 (1992).
[14] S.C. Rae, Opt. Commun. **97**, 25 (1993).
[15] T. Auguste *et al.*, Opt. Commun. **89**, 145 (1992).
[16] P. Monot *et al.*, J. Opt. Soc. Am. B **9**, 1579 (1992).
[17] E.E. Fill, J. Opt. Soc. Am. B **11**, 2241 (1994).
[18] C. Leblanc *et al.*, Opt. Lett. **18**, 140 (1993).
[19] J.R. Marquès *et al.*, Phys. Plasmas **5**, 1167 (1998); P. Chessa *et al.*, Phys. Plasmas **5**, 3451 (1998).
[20] P. Mora and T.M. Antonsen, Jr., Phys. Plasmas **4**, 217 (1997).
[21] A.M. Perelomov *et al.*, JETP Lett. **23**, 924 (1965).
[22] M.V. Ammosov *et al.*, JETP Lett. **64**, 1191 (1986).
[23] S. Augst *et al.*, J. Opt. Soc. Am. B **8**, 858 (1991).
[24] M. Lontano *et al.*, Phys. Scr. **T63**, 141 (1996).